Desert dust outbreaks over Mediterranean basin: a modeling, observational, and synoptic analysis approach

Hindawi Publishing Corporation
Advances in Meteorology
Volume 2012, Article ID 246874, 14 pages
doi:10.1155/2012/246874

Research Article

Desert Dust Outbreaks over Mediterranean Basin: A Modeling, Observational, and Synoptic Analysis Approach

F. Calastrini,[1,2] F. Guarnieri,[1,2] S. Becagli,[3] C. Busillo,[1] M. Chiari,[4] U. Dayan,[5] F. Lucarelli,[4,6] S. Nava,[4] M. Pasqui,[2] R. Traversi,[3] R. Udisti,[3] and G. Zipoli[2]

[1] *LaMMA Consortium, Laboratory of Monitoring and Environmental Modeling for the Sustainable Development, Via Madonna del Piano 10, 50019 Sesto Fiorentino, 50019 Sesto Fiorentino, Italy*
[2] *IBIMET, National Research Council, Via G. Caproni 8, 50145 Florence, Italy*
[3] *Department of Chemistry, University of Florence, Via della Lastruccia 3, 50019 Sesto Fiorentino, Italy*
[4] *INFN, National Institute of Nuclear Physics, Via G. Sansone 1, 50019 Sesto Fiorentino, Italy*
[5] *Department of Geography, The Hebrew University of Jerusalem, Jerusalem 91905, Israel*
[6] *Department of Physics and Astronomy, University of Florence, Via G. Sansone 1, 50019 Sesto Fiorentino, Italy*

Correspondence should be addressed to F. Calastrini, calastrini@lamma.rete.toscana.it

Received 9 March 2012; Accepted 19 June 2012

Academic Editor: Pawan Gupta

Dust intrusions from African desert regions have an impact on the Mediterranean Basin (MB), as they cause an anomalous increase of aerosol concentrations in the tropospheric column and often an increase of particulate matter at the ground level. To estimate the Saharan dust contribution to PM_{10}, a significant dust intrusion event that occurred in June 2006 is investigated, joining numerical simulations and specific measurements. As a first step, a synoptic analysis of this episode is performed. Such analysis, based only on meteorological and aerosol optical thickness observations, does not allow the assessment of exhaustive informations. In fact, it is not possible to distinguish dust outbreaks transported above the boundary layer without any impact at the ground level from those causing deposition. The approach proposed in this work applies an ad hoc model chain to describe emission, transport and deposition dynamics. Furthermore, physical and chemical analyses (PIXE analysis and ion chromatography) were used to measure the concentration of all soil-related elements to quantify the contribution of dust particles to PM_{10}. The comparison between simulation results and in-situ measurements show a satisfying agreement, and supports the effectiveness of the model chain to estimate the Saharan dust contribution at ground level.

1. Introduction

Aerosols have direct and indirect effects on global climate [1], altering the radiative balance of the Earth-atmosphere system [2–4] and changing the microphysical and the radiative properties of clouds. In fact, aerosol particles can act as cloud condensation nuclei, modifying cloud lifetime and amount [3–5]. The mineral dust from desert areas, which represent a great source of aerosol injected into the atmosphere, suppresses precipitation in thin low-altitude clouds [6–8]. In addition, dust deposition can modify the ocean biogeochemical cycle, providing an important source of micronutrients [9]. It has also an impact on terrestrial ecosystems, providing nutrients as phosphorus to the soil [10]. Saharan desert is one of the most important sources of mineral dust [11], which has a considerable impact both at the global [12] and at the regional scale, as the Mediterranean Basin (MB) [13].

More specifically, Saharan dust outbreaks can cause an anomalous rise of PM_{10} concentrations over large parts of the MB, with impacts on Spain, Greece, and Italy [14–16]. The exceedance of daily thresholds established by the European Union (Directive 2008/50/EC) may depend not only on human emissions but also on the mineral dust contribution. The same directive includes the possibility of removing exceedances due to natural sources, such as atmospheric resuspension or the transport of natural particles from dry regions. Although the assessment of a recognised procedure to quantify and subtract the effective Saharan dust contribution to PM_{10} concentration levels is

still under discussion, preliminary guidelines are proposed in a working paper of the European Commission (http://www.ec.europa.eu/environment/air/quality/legislation/pdf/sec_2011_0208.pdf), mainly following the approach reported in Escudero et al. [17].

The method proposed in the European guidelines suggests to combine the use of satellite retrievals, model systems, and PM_{10} measurements at the ground level. The meteorological analysis (ECMWF http://www.ecmwf.int/) checks the evolution of synoptic systems prone to the generation of strong gradient winds able to transport dust plumes from North Africa towards Europe. The satellite observations (http://oceancolor.gsfc.nasa.gov/SeaWiFS/HTML/dust.html) and the aerosol index (TOMS http://toms.gsfc.nasa.gov/ozone/ozone_v8.html) can be useful in the detection of the dust episode and in the identification of the area affected by the plumes. Daily results of numerical models (e.g., SKIRON http://forecast.uoa.gr/, BSC-DREAM http://www.bsc.es/projects/earthscience/BSC-DREAM/ and NAAPs http://www.nrlmry.navy.mil/aerosol/) can be checked to identify the occurrence and the duration of the dust episode. Using only satellite observations and model simulations of aerosol optical thickness, it is not possible to clearly distinguish episodes that involve dust transport above the boundary layer without any impact at the ground level from those that cause dust deposition. For this reason, the European guidelines also require an analysis of PM_{10} mass concentration, which is routinely measured at the ground level by air quality station networks. Distinguishing between the Saharan dust contribution is not trivial since the PM_{10} concentration may be contributed by many different sources [16]. In a near future, the results of this method will be provided by GMES-Atmosphere service (http://www.gmes-atmosphere.eu/).

Within this framework, a study of Saharan dust intrusions over the MB is proposed, focusing on the deposition mechanism to assess the dust impact at the ground level. For this reason, a comprehensive model chain is configured to reconstruct the dynamic evolution of the Saharan desert dust. Numerical models play an important role in the description of the process of dust emission, transport, and deposition from desert zones. It is possible to reconstruct the spatial distributions of the dust with a good description of the vertical concentration profile. To characterise the PM_{10} mass concentration and composition at the ground level, the model-based analysis is complemented by physical and chemical analyses of the PM_{10} sampled in different sites. In particular, the concentration of all soil-related elements is measured by PIXE (Particle-Induced X-ray Emission) to assess the mineral dust concentration. The ionic composition is also used as ancillary data to subtract the sea-salt contributions to Na and Mg. Because the impact of desert dust is well characterised by an increase of all soil-related elements (and by changes in elemental ratios), this approach is useful for assessing the real impact of dust episodes on PM_{10}. The measurement of all crustal elements may allow a quantitative assessment of the desert dust contribution, which is more accurate with respect to estimations that may be obtained simply by the analysis of PM_{10} mass concentration data. In addition to the specific quantitative information obtained by the PM_{10} measurements in the selected sampling sites, the integrated use of model simulations and in situ experimental data may provide an overall picture of the mineral dust distribution.

This approach, which joins numerical simulations and specific measurements, is employed to study the impact of Saharan dust event of June 2006, a month characterised by significant dust outbreaks over the MB [18, 19]. Since at the moment, the GMS-Atmosphere service is not operational, a preliminary analysis of this long spell is conducted using the available data as the synoptic meteorological data from NCEP, the satellite observation images (MODIS/AQUA, MODIS/TERRA http://modis.gsfc.nasa.gov/), and the aerosol index (TOMS). The global model GOCART (http://disc.sci.gsfc.nasa.gov/ges-News/gocart_data_V006), developed by the Georgia Institute of Technology-Goddard to simulate aerosol optical thickness [20, 21], is used to integrate the satellite data. The HYSPLIT model (Hybrid Single Particle Lagrangian Integrated Trajectory model, http://ready.arl.noaa.gov/HYSPLIT.php) is used to generate backward trajectories to trace back the sources of the air masses at different levels and for different hours of the day.

The results of model chain, configured to describe the spatiotemporal evolution of this specific dust outbreak, are compared with GOCART data. Physical and chemical analyses are conducted on PM_{10} samples collected from three sites in central Italy (Tuscany). Finally, the numerical simulation results are compared with these specific measurements to evaluate the effectiveness of the model chain in the quantitative estimation of the Saharan dust contribution at the ground level.

2. Instruments and Methods

2.1. The Model Chain. The natural phenomena involved in the dust cycle in the atmosphere consist of two major physical processes: a wind stress lifting mechanism enabling the dust particles to rise up from bare soil surfaces and then the transport and deposition of this mineral dust [22–24]. To provide regional characteristics of Saharan dust intrusion over the MB, an atmospheric emission and dispersion model chain is developed. The model chain is based on three different modules: the atmospheric, dust emission, and transport/deposition modules. The Regional Atmospheric Modeling System (RAMS) [19], used by CNR-IBIMET in operational mode [25–27], provides the input data for the other modules. The DUST Emission Model (DUSTEM), specifically developed for this aim, simulates the dust emission from the desert. The Comprehensive Air quality Model with extensions (CAMx) (http://www.camx.com/home.aspx) takes the meteorological inputs from RAMS and the emission rate from DUSTEM [28], providing the dynamical transport and deposition of the dust particles.

This section describes the model chain configuration used for this case study from 1 June to 5 July 2006.

Table 1: Features of the four typical dust particles.

Type	Name	Typical particle diameter (μm)	Typical particle radius (μm)	Particle density (g/cm^3)	Erodible fraction
Clay	CCR1	**01-02**	**0.73**	**2.50**	**0.08**
Silt, small	CCR2	**02–20**	**6.1**	**2.65**	**1.00**
Silt, large	CCR3	20–50	18	2.65	1.00
Sand	CCR4	50–100	38	2.65	0.12

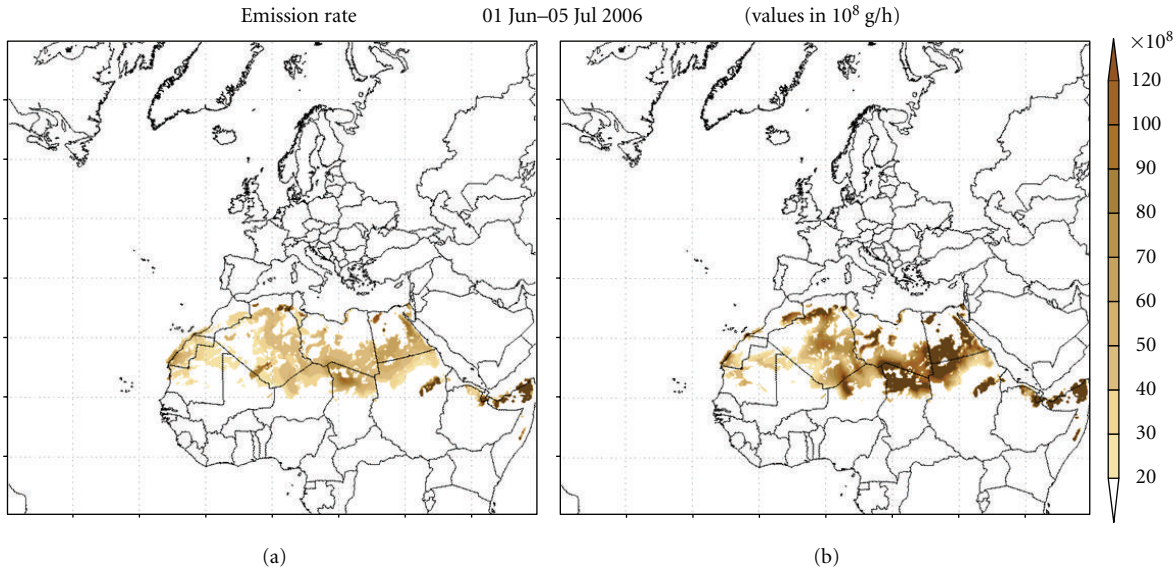

Figure 1: Emission rate, cumulated on the period 01–05 June 2006 for the first dimensional class (a) and for the second dimensional class (b).

2.2. The Regional Atmospheric Modeling System (RAMS). The RAMS 6.02 version is run over a domain including a large part of the Northern Hemisphere and performed by parallel computing. The initial and boundary atmospheric conditions need to be set as well as the forcing data during the period of simulation. To address these necessities, the Reanalysis2 dataset [29], with a 2.5-degree horizontal resolution, is employed. In particular, the geopotential height, temperature, relative humidity, and zonal and meridional wind component fields are used and forced as boundary conditions every 6 hours throughout the simulation period. The Kain-Fritsch convective scheme is also adopted. The configuration is set with the following features: the domain is centered on 40°N–5°E, with 200 × 80 grid points, 32 sigma vertical levels (with a stretching factor to obtain a greater resolution near the soil and a lesser one above 2000 m) and 11 soil levels. The horizontal resolution is 0.54 degrees, and the time step is 120 seconds, with a temporal output of 1 hour.

2.3. The Dust Emission Model (DUSTEM). Dust emissions are estimated by developing an ad hoc model called the DUST Emission Model (DUSTEM) [28]. This model estimates dust emission rates using empirical relationships based on soil texture and friction velocity [30]. DUSTEM can take into account four different soil types: clay, small silt, large silt, and sand [30, 31]. The main features of these classes are shown in Table 1. For the selected case study, only the first two dimensional classes, clay and small silt, are considered because they are the only ones involved in long-range transport [31]. DUSTEM takes the soil information from the GLC2000 land cover [32] and FAO Textural Map [33] as input data to obtaining the bare soil map. The hourly meteorological fields (soil moisture and friction velocity) are provided by the RAMS model. The computational domain, in Polar Stereographic coordinates (with the pole at 40 degrees north and 5 degrees east), is formed by 380 × 340 cells with a 30 km resolution to provide the input data to CAMx with a temporal resolution of 1 hour. The maps of emission rates cumulated on the whole simulation period, relative to the first and second soil types, are shown in Figure 1.

2.4. The Comprehensive Air Quality Model (CAMx). The Comprehensive Air quality Model (CAMx), developed by ENVIRON International Corporation California, is an Eulerian photochemical dispersion model that allows for an integrated "one-atmosphere" assessment of gaseous and particulate air pollution over many scales, ranging from urban to superregional (http://www.camx.com/home.aspx). CAMx simulates the dispersion, chemical reactions, and removal of pollutants in the troposphere by solving the pollutant continuity equation for each species. The aerosol deposition is handled by adopting the algorithm of S. A. Slinn and W. G. N. Slinn [34] and Seinfeld and Pandis [35] for the dry and wet deposition, respectively. To simulate the transport and deposition of mineral dust, the chemical module is switched off in this study. The meteorological input data are provided by RAMS, and the emission rates of clay and small silt types are provided by DUSTEM (Table 1). The initial and boundary conditions are set to zero. To consider the atmospheric dust loading, the simulation starts

on 1 June, some days in advance of the outbreak over Europe. The horizontal computational domain is the same as that used for DUSTEM. There are 18 vertical levels, from 10 m to 10,500 m, with a finer resolution near the ground. The concentration outputs for clay and small silt soil types are provided with a temporal resolution of 1 hour.

2.5. PM_{10} Sampling and Analysis. To characterise the PM_{10} mass concentration and composition at the ground level, the concentration of all soil-related elements is measured by PIXE to assess the mineral dust concentration [36–40]. The simultaneous detection, with high sensitivity, of all the elements that compose mineral dust makes PIXE highly effective for these investigations. A simultaneous increase in the concentration of all crustal elements is indeed a first indication of the occurrence of dust events; clearly, it is a stronger signature than the increase of the PM mass concentration, which may be due to many other sources, both natural and anthropogenic. However, an increase of crustal element concentrations may also be due to local soil dust resuspension: in this context, the analysis of changes in elemental ratios may help distinguish between these two kinds of events. Moreover, when the aerosol is sampled at more than one site, the observation of a simultaneous increase of soil-related elements at the different sites may also suggest the impact of long-range transported soil dust affecting a wide area, while the observation of different patterns from site to site clearly hints at the contribution of local sources.

2.6. PM_{10} Sampling. Aerosol samples are collected on 47 mm Teflon filters on a daily basis (from midnight to midnight) using low-volume (2.3 m^3/h) sequential samplers (HYDRA Dual Sampler, FAI Instruments) equipped with a PM_{10} inlet in accordance with the European rule EN 12341.

The PM_{10} daily mass concentrations are obtained by weighing the filters with an analytical balance (sensitivity 1 μg) before and after the sampling, always after a storage period (48 hours) in a temperature and humidity controlled room with an ambient temperature $T = (20 \pm 1)^{\circ}$C and a relative humidity RH = (50 ± 5)%. Electrostatic effects are avoided by using a deionising gun.

In particular, a comprehensive dataset of PM_{10} measured concentrations and composition at the ground level is obtained in the framework of the PATOS project, the first extensive field campaign for PM_{10} characterisation in Central Italy (Tuscany), which was supported by the Regional Government (http://servizi.regione.toscana.it/aria/index.php?idDocumento=18348). PM_{10} samples are collected from September 2005 to September 2006 at six sampling sites in Tuscany that are representative of different types of areas: Florence (urban background), Prato (urban traffic), Capannori-Lucca (urban background), Arezzo (urban traffic), Grosseto (urban background), and Livorno (suburban background). In this field campaign, the three available samplers are used to collect the PM_{10} data in the six sites previously cited. These samplers are moved every 15 days from three sampling sites (Arezzo, Prato, and Livorno) to the other three (Florence, Capannori-Lucca, and Grosseto). In this way, data relative to the long-range transport dust intrusion of June and the background level due to local dust resuspension is sampled.

2.7. PM_{10} Compositional Analysis. The PM_{10} samples are analysed by Particle-Induced X-ray Emission (PIXE) to determine the aerosol elemental composition and, in particular, the concentrations of all the main soil-related elements (Na, Mg, Al, Si, K, Ca, Ti, Mn, Fe, and Sr). The same samples are also analysed by ion chromatography (IC) to assess the soluble fraction of inorganic ions, specifically the Na^+ and Mg^{2+} concentrations. These values are used to determine the sea-salt contributions to Na and Mg to be subtracted for the calculation of the soil dust fraction of these elements.

The PIXE measurements are performed at the 3 MV Tandetron accelerator of the LABEC laboratory of INFN in Florence using the external beam setup dedicated to environmental applications [39, 41]. For this case study, each sample is irradiated for ~500 s with a 3.2 MeV proton beam with an intensity of ~5 nA over a spot of ~2 mm^2. During irradiation, the filter is moved in front of the beam so that most of the area of the deposit is analysed. The PIXE spectra are fitted using the GUPIX code [42] and elemental concentrations are obtained via a calibration curve from a set of thin standards (Micromatter Inc.). The minimum detection limits (MDLs) are ~10 ng/m^3 for low-Z elements and ~1 ng/m^3 for medium-high-Z elements. The elemental concentration uncertainty is determined by taking into account the independent uncertainties on the standard sample thickness (±5%), the aerosol deposition area (±2%), the airflow (±2%), and the X-ray counting statistics (from ±2 to ±20% or higher when concentrations approach MDLs).

Ion analysis is performed on the water extract obtained from a quarter of each Teflon filter. Each sample is analysed for cations (Na^+, NH_4^+, K^+, Mg^{2+}, and Ca^{2+}), inorganic anions (F^-, Cl^-, NO_3^-, and SO_4^{2-}), and some organic anions (methanesulphonate (MSA), acetate, formate, glycolate, and oxalate) by 3 Dionex ion chromatographic systems operating in parallel under the working conditions summarised by Becagli et al. [43]. The detection limits are several orders of magnitude lower than the concentrations found in these samples. The uncertainty is mainly determined by the ion chromatography accuracy, which is typically ±5%.

3. Results and Discussion

3.1. Synoptic Conditions Featuring the Dust Outbreak. The synoptic atmospheric conditions favourable for dust raising are those associated with air mass advection coming from Northern Europe or the Balkans regions and heading towards Algeria, Libya, and Egypt up to Chad [44]. These air masses are characterised by strong and constant wind in the lower layers. The associated thermal gradient has two important effects for dust emissions: the first is the increase of the soil friction in correspondence with the air mass front due to the acceleration of the thermal wind; the latter is the reduction of

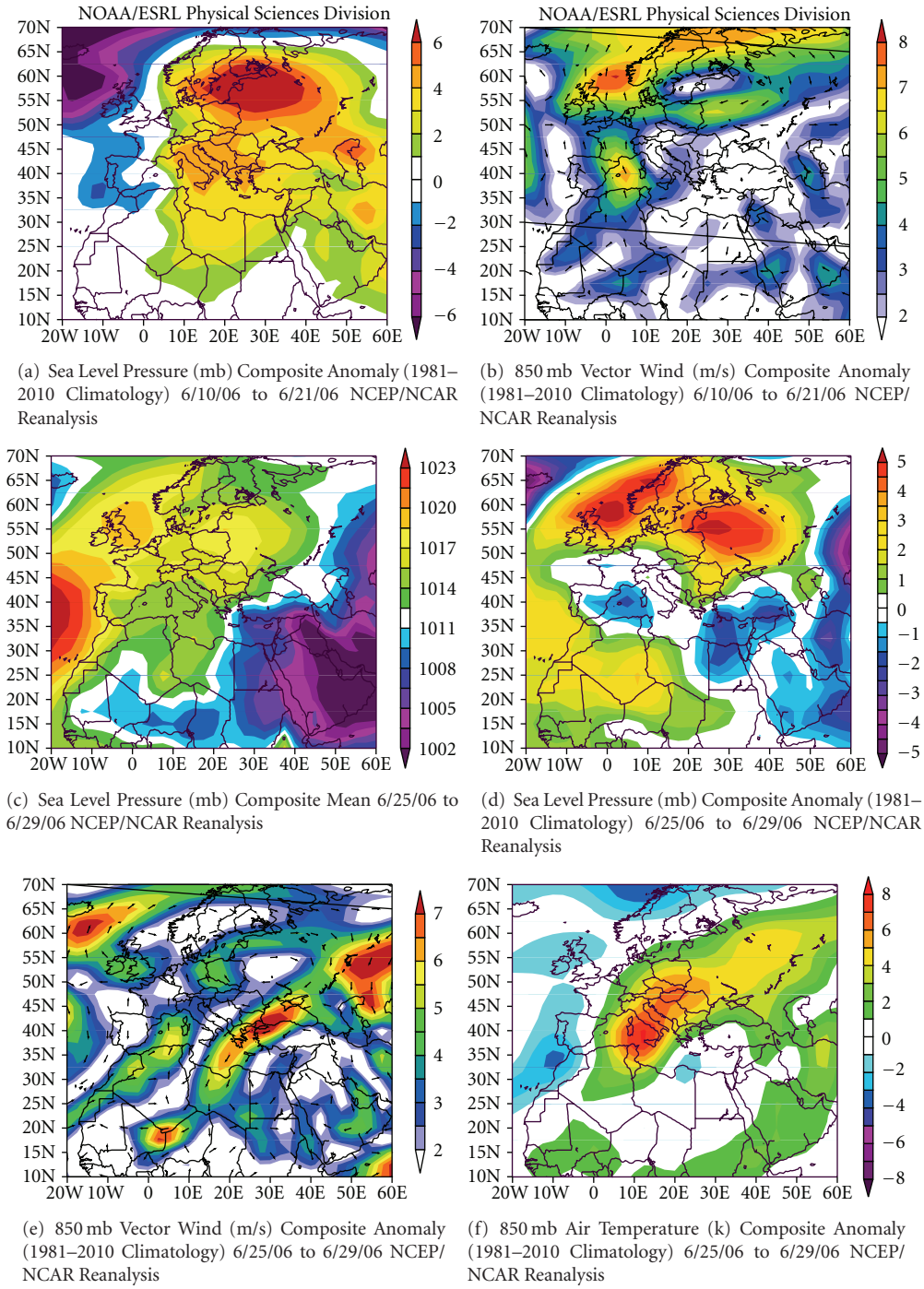

(a) Sea Level Pressure (mb) Composite Anomaly (1981–2010 Climatology) 6/10/06 to 6/21/06 NCEP/NCAR Reanalysis

(b) 850 mb Vector Wind (m/s) Composite Anomaly (1981–2010 Climatology) 6/10/06 to 6/21/06 NCEP/NCAR Reanalysis

(c) Sea Level Pressure (mb) Composite Mean 6/25/06 to 6/29/06 NCEP/NCAR Reanalysis

(d) Sea Level Pressure (mb) Composite Anomaly (1981–2010 Climatology) 6/25/06 to 6/29/06 NCEP/NCAR Reanalysis

(e) 850 mb Vector Wind (m/s) Composite Anomaly (1981–2010 Climatology) 6/25/06 to 6/29/06 NCEP/NCAR Reanalysis

(f) 850 mb Air Temperature (k) Composite Anomaly (1981–2010 Climatology) 6/25/06 to 6/29/06 NCEP/NCAR Reanalysis

Figure 2: Meteorological fields from NCEP/NCAR Reanalysis. The anomalies are evaluated on the climatology 1981−2010. (a) Sea level pressure anomaly for 10−21 June 2006, (b) 850 mb wind vector anomaly for 10−21 June 2006, (c) mean sea level pressure for 25−29 June 2006, (d) sea level pressure anomaly for 25−29 June 2006, (e) 850 mb wind vector anomaly for 25–29 June 2006, and (f) 850 mb air temperature anomaly for 25−29 June 2006.

the soil moisture content due to the positive surface, which favours the raising of dust.

Once the dust is raised above the boundary layer, a strong circulation between 850 and 700 hPa is necessary to transport the dust far from the emission area. Throughout the year, massive airborne plumes of desert dust from the Sahara and surrounding regions are exported to the tropical Atlantic Ocean and the Mediterranean Sea. The majority of the dust intrusions over the MB are usually associated with the passage of either a cold or a warm low-pressure system. Saharan depressions develop most readily when a Polar or Arctic air mass from the northwest (Maritime Polar or Maritime Arctic) or northeast (Continental Polar or Continental Arctic) flows behind the dry desert air [45].

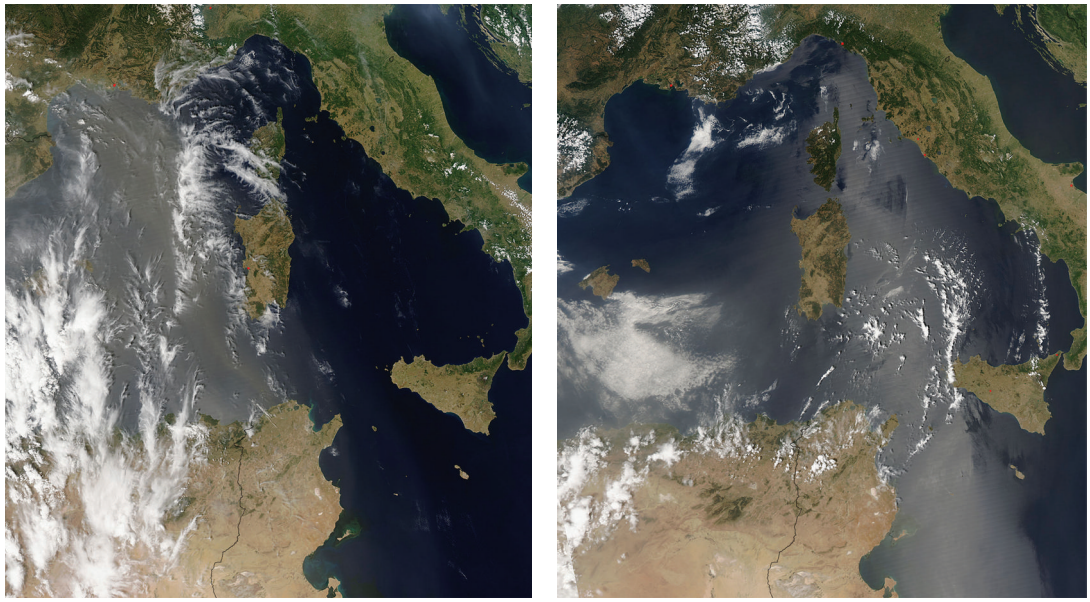

(a) (b)

Figure 3: MODIS/AQUA images for 15 June (a) and 26 June (b) 2006.

To analyse the synoptic circulation over the Mediterranean area during the case study of June 2006, the sea level pressure, air temperature, and wind fields are investigated using a daily NCEP Reanalysis database provided by the NOAA/OAR/ESRL PSD (website at http://www.esrl.noaa.gov/psd/). The anomalies are calculated with respect to the long-term mean (LTM) period of 1981–2010. The screening of 6-hourly sea level pressures (SLPs), wind vectors, and air temperatures at different pressure levels reveals major dust outbreaks originating from the North African deserts towards Europe and provides insight into their temporal evolution. The means and anomalies of these 3 meteorological fields, compared with their LTMs, are calculated and discussed as follows.

From 10 to 21 June 2006, the average SLP distribution over the MB highlights a pronounced high-pressure system over the West Mediterranean Basin (4 mb in excess of the LTM for this period) and a low-pressure system over southern Algeria (Figure 2(a)). The West Mediterranean (WM), exposed to the influence of both systems, is subjected to the generation of SE gradient winds at 850 hPa, resulting in this episode being 6-7 m s^{-1} stronger than the normal wind flow over this region (Figure 2(b)). On 23 June, an Atlantic perturbation advances toward the Central Mediterranean area and weakens the SW flux and the dust transport over Italy. The following period, from 25 to 29 June 2006, is characterised by an extension of the Azorean ridge deep into northern Europe together with a weakening of the African Monsoon over southern Algeria (Figure 2(c)). This synoptic configuration yields a negative anomaly of 1-2 hPa over the whole MB (Figure 2(d)) with one of its two lowest pressure cores centred over the North Western African coast. This low-pressure system induces a cyclonic flow at shallow atmospheric layers over the WM, characterised by anomalous strong Westerlies over this region accompanied by stronger than usual SE winds over Sardinia and Corsica (Figure 2(e)). This counterclockwise flow led to a positive anomaly in air temperature over the WM and the Central Mediterranean (Figure 2(f)).

The satellite observations, as shown in Figure 3(a) for 15 June, and the TOMS aerosol index reveal air masses transporting significant amounts of dust over large parts of the WM originating from southern Algeria and SW Africa. The TOMS data and the AQUA satellite observations (Figure 3(b)) for 27 June 2006 show the plume of dust originating from SW Algeria migrating in a cyclonic direction path through Sicily and Central Italy, crossing Sardinia and Corsica on its way to the Genoa Bay and eastern Spain.

The GOCART dust aerosol optical depth (AOD) daily maps are also used to follow the evolution of the dust outbreak on a daily basis [20]. As an example, Figure 4 represents the AOD for 15, 21, 24, and 26 June, showing the dust transport over the MB.

Finally, the Lagrangian trajectory HYSPLIT (Hybrid Simple Particle Lagrangian Integrated Trajectory) model is used to generate backward trajectories to trace back the sources of the air masses at different levels and for different hours of the day. Figure 5 shows the trajectories ending in Florence on 29 June 2006 at three different levels of A.G.L. (500, 1000, and 1500 m) starting from Northern Africa.

3.2. Numerical Simulations of Mineral Dust Events. The model chain is performed from 1 June to 5 July 2006. An analysis of the model results, based on the daily vertically integrated dust concentrations for the particle size 1–20 μm (as a sum of clay and small silt soil types), is presented. From 6 June, the Saharan desert dust is transported to the Iberian Peninsula, and in the following days, the dust reaches Northern Europe (France, UK, and Norway). From 16 to 22 June, a large area ranging from the West MB

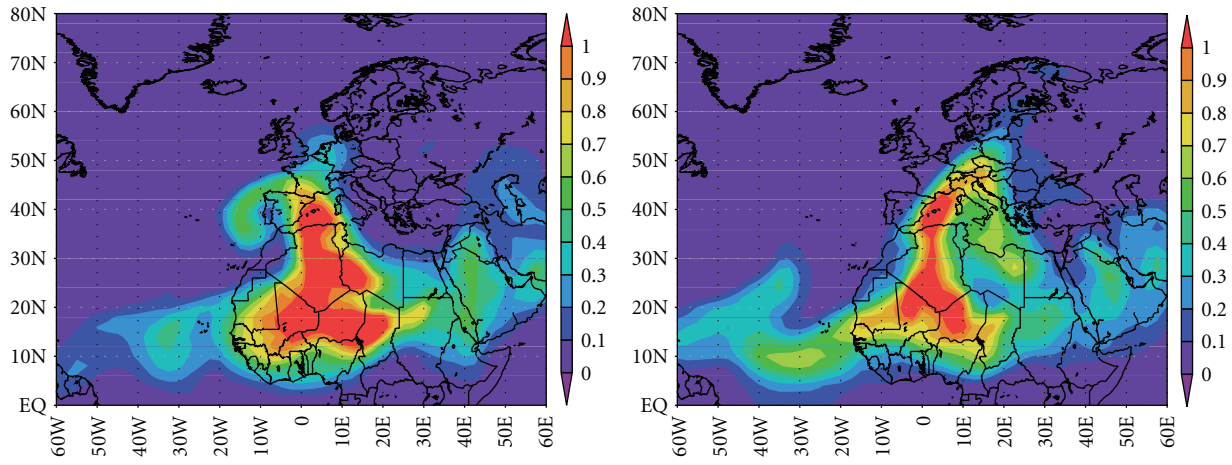

(a) G4P0_1DA_2D_du_aot.006 Dust Aerosol Column Optical Depth (550 nm) (untiless) (15Jun2006)

(b) G4P0_1DA_2D_du_aot.006 Dust Aerosol Column Optical Depth (550 nm) (untiless) (21Jun2006)

(c) G4P0_1DA_2D_du_aot.006 Dust Aerosol Column Optical Depth (550 nm) (untiless) (24Jun2006)

(d) G4P0_1DA_2D_du_aot.006 Dust Aerosol Column Optical Depth (550 nm) (untiless) (26Jun2006)

Figure 4: Dust Aerosol Column Optical Depth (550 nm) from GOCART aerosol model data V006, for the 15th of June (a), 21st of June (b), 24th of June (c), and 26th of June (d) 2006.

to the Scandinavian Peninsula and Russia is affected by a mineral dust intrusion that also reached Italy. In particular, during 17 and 18 June, Spain, France, Switzerland, Germany, Italy, and the Balkan Peninsula are affected by elevated dust concentrations. During 23 and 24 June, the Italian peninsula experienced a decrease of dust concentration due to a newly formed cyclone coming from the Atlantic Ocean, which interrupted the southwestern flux over Italy. Afterwards, the transport mechanism proceeds again until the first days of July, although the concentration values are lower than those in the previous period. Figure 6 shows the daily vertically integrated dust concentrations for 15, 21, 24, and 26 June 2006. The qualitative comparison between these simulation results, the satellite retrievals, and the TOMS index data show a good agreement with the location of the zones that encountered dust intrusions. Furthermore, the GOCART dust aerosol optical depth daily maps are compared with simulation's results for the whole period, from 1 June to 5 July, to evaluate whether the model chain correctly reproduces the dust event. There is temporal and spatial agreement between the CAMx and GOCART results, as shown in Figures 4 and 6.

The RAMS/DUSTEM/CAMx model chain, configured with a finer resolution than GOCART, provides more detailed information on the vertical distribution of dust concentration and on the deposition at the ground level. In fact, the vertical sections of the mean daily dust concentration, for example at latitude 43.78°N (Florence), show dust advancing towards Spain and France, at both low and high levels up to 5000–7000 meters. The greatest dust concentration over Europe is reached during the period of 15–22 June between 1000 and 8000 metres, whereas under the boundary layer, the concentrations are lower (30–40 μg/m^3 versus 200–500 μg/m^3) (Figure 7). During 23-24 June, the Atlantic cyclonic flow temporarily interrupts the dust transport over Tuscany. On 25 June, the dust is transported only above the boundary layer without deposition. Observing the daily modeled dust concentration at the ground level, a strong decrease is evident, as also proved by ground measurements (next paragraphs). Such information cannot be obtained

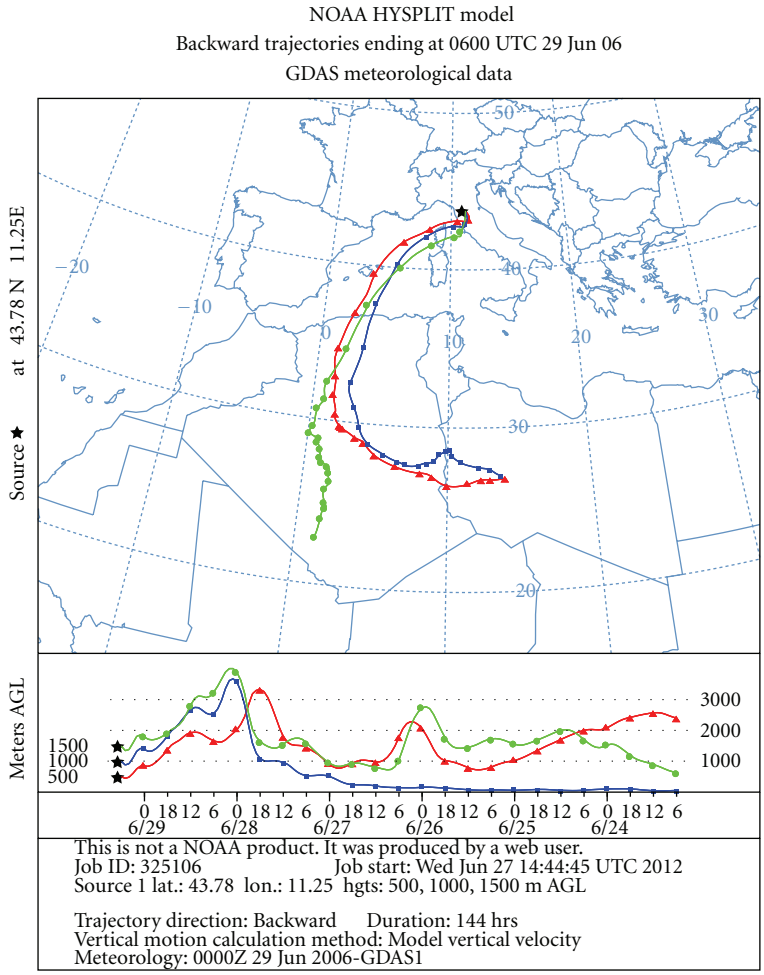

Figure 5: 144 hr back trajectories calculated by the HYSPLIT transport model (NOAA Air Resource Laboratory). The trajectories end in Florence at three different levels above the ground (10, 100, and 500 m) on the 29th of June 6 : 00 UTC.

from the results based on the daily vertically integrated dust concentrations or from an analysis of the optical depth maps. Finally, in the last part of the episode (26 June–2 July), the vertical extent of the dust concentration is lower, reaching 5000–6000 meters, and the dust event is less intense (Figure 7).

3.3. Chemical and Physical Analysis. During the month of June 2006, the concentrations of all the main crustal elements (Na, Mg, Al, Si, K, Ca, Ti, Mn, Fe, and Sr) show a clear increase together with the WM Saharan intrusion simultaneously in all sampling sites in Tuscany (Figure 8). The concentrations start to increase from 18 June and return to background values on 2 July. The time series show a two-peak shape, with a central minimum (24-25 June). As mentioned previously, the samplers are moved from three sampling sites to the other three every 15 days: in June, these displacements occurred on the 14th and 29th. Consequently, most of the episode (18–28 June) is measured in Florence, Capannori-Lucca, and Grosseto, one day (28 June) is missed, and the last part of the event (30 June–2 July) is observed in Arezzo, Livorno, and Prato. The average concentration values of the crustal elements during the episode are 2–4 times higher than their background concentrations. Al, Si, and Ti show a higher increase: their maximum concentration values during the episode ($\sim 2.5\,\mu g/m^3$, $\sim 6.0\,\mu g/m^3$, and $\sim 0.2\,\mu g/m^3$) are approximately 6 times higher than their background values.

Elemental ratios among the crustal elements also show significant changes, thus further reinforcing the Saharan intrusion hypothesis. For example, the Si/Al ratio mean and standard deviation during the episode is 2.3 ± 0.1 in Florence, 2.4 ± 0.1 in Capannori-Lucca, and 2.2 ± 0.1 in Grosseto, while the same ratios calculated for the other days (i.e., excluding the days of the episode) are ~15% higher (2.7 ± 0.2, 2.8 ± 0.2, and 2.5 ± 0.2, resp.); the Ti/Fe ratio during the episode is 0.08 ± 0.01 in Florence, 0.08 ± 0.01 in Capannori-Lucca, and 0.09 ± 0.01 in Grosseto, while it is ~50–70% lower during the other days (0.04 ± 0.01, 0.05 ± 0.01, and 0.06 ± 0.01, resp.); the Al/Ca ratio during the episode is 0.41±0.07 in Florence, 0.49 ± 0.11 in Capannori-Lucca, and 0.57 ± 0.12 in Grosseto, while it is ~40–80% lower during the other days (0.29 ± 0.06, 0.28 ± 0.07, and 0.32 ± 0.08, resp.). Similar results are found at two remote sites of Northern and Central Italy by Bonelli et al. [36]. In both studies, a decrease of the Si/Al ratio and an

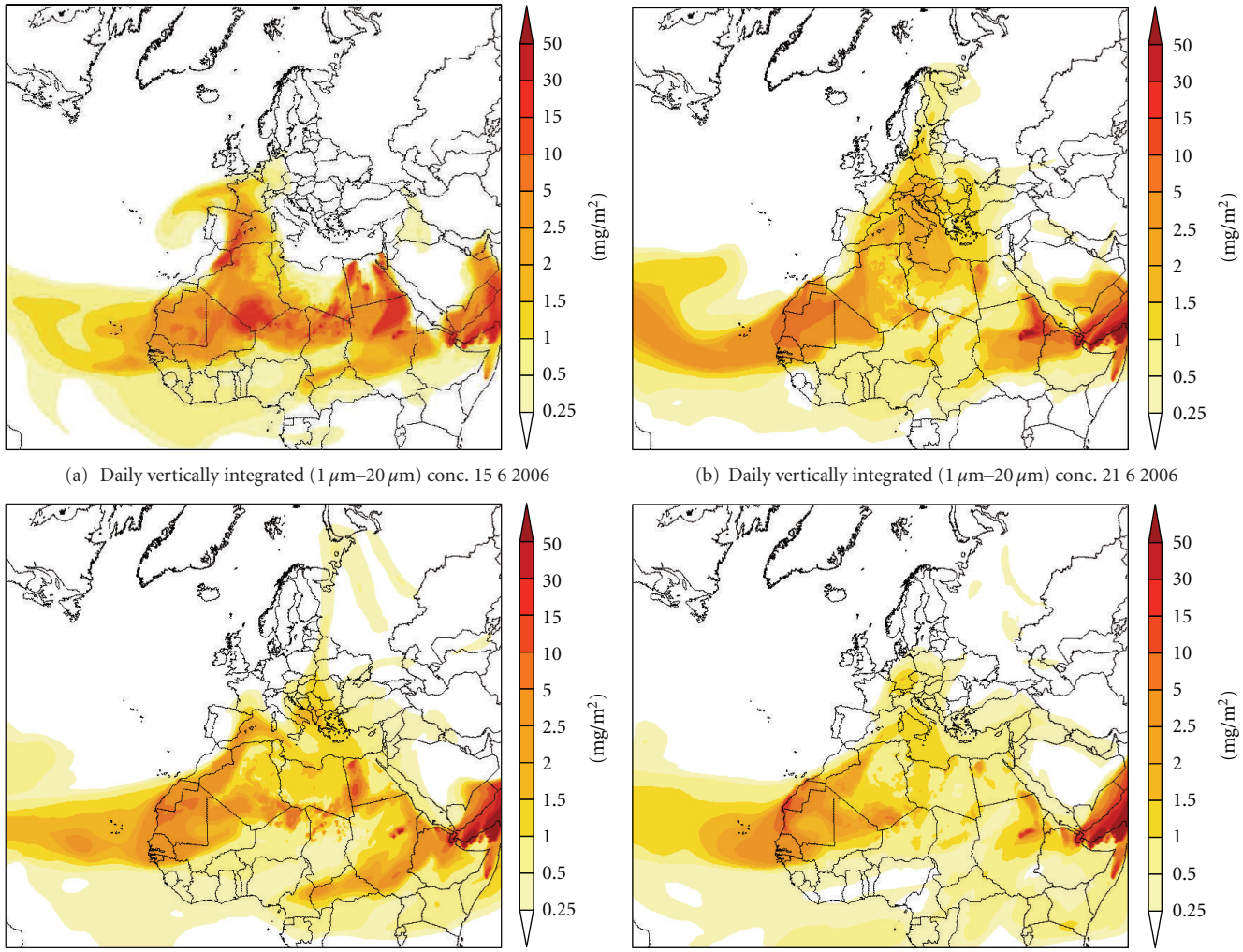

(a) Daily vertically integrated (1 μm–20 μm) conc. 15 6 2006

(b) Daily vertically integrated (1 μm–20 μm) conc. 21 6 2006

(c) Daily vertically integrated (1 μm–20 μm) conc. 24 6 2006

(d) Daily vertically integrated (1 μm–20 μm) conc. 26 6 2006

FIGURE 6: Daily vertically integrated dust concentration for 15th of June (a), 21st of June (b), 24th of June (c), and 26th of June 2006 (d).

increase of the Ti/Fe and Al/Ca ratios are indicated as highly representative fingerprints of African dust transport events. Their reported values for the Si/Al ratio during these events (and during days not affected by Saharan intrusions), that is, 2.3-2.4 (2.7-2.8), match well with those found in this study. The Si/Al ratio decrease may be explained by a higher contribution during the Saharan intrusions of agglomerated clay minerals with respect to bulk crustal material, while the increase of the Ti/Fe and Al/Ca ratios may be ascribed to an iron and Ca enrichment in local soil dust.

An estimation of the soil dust component may be calculated as the sum of the contributions of the main oxides of all the crustal elements (Na_2O_2, MgO, SiO_2, Al_2O_3, TiO_2, K_2O, CaO, and Fe_2O_3):

$$[\text{soil dust}] = 1{,}7\,[\text{nssNa}] + 1{,}67\,[\text{nssMg}] + 1{,}89\,[\text{Al}] + 2{,}14\,[\text{Si}] + 1{,}2\,[\text{K}] + 1{,}4\,[\text{Ca}] + 1{,}43\,[\text{Fe}] + 1{,}67\,[\text{Ti}], \quad (1)$$

where [nssNa] and [nssMg] are the concentrations of "non-sea-salt" Na and Mg (i.e., excluding the sea-salt contribution).

This expression may overestimate soil dust due to the contribution of other sources, such as biomass burning (for K), traffic, and other anthropogenic sources for Fe, and Ca. During the studied period the enrichment factors of K, Fe, and Ca (with respect to Al using the crust composition reported in Mason [18]) turn out to be low, suggesting the absence of strong anthropogenic contributions. Consequently, no correction is applied to the calculation of their contribution to soil dust. The sea-salt fractions of Na and Mg are calculated using the IC data, as the measured Na^+ and Mg^{2+} soluble ion concentrations may actually be considered good estimations for these contributions.

The daily time series of soil dust concentration, calculated as reported above, are shown in Figure 8. During the Saharan intrusion, values of 20–30 $\mu g/m^3$ are reached, to be compared with background values of the order of a few $\mu g/m^3$. The Saharan dust contribution, for all the days of the episode, is estimated by subtracting the background soil dust concentration, which is calculated, site by site, as an average from mid-May to the end of July, excluding the Saharan intrusion days. The results together with the PM_{10}

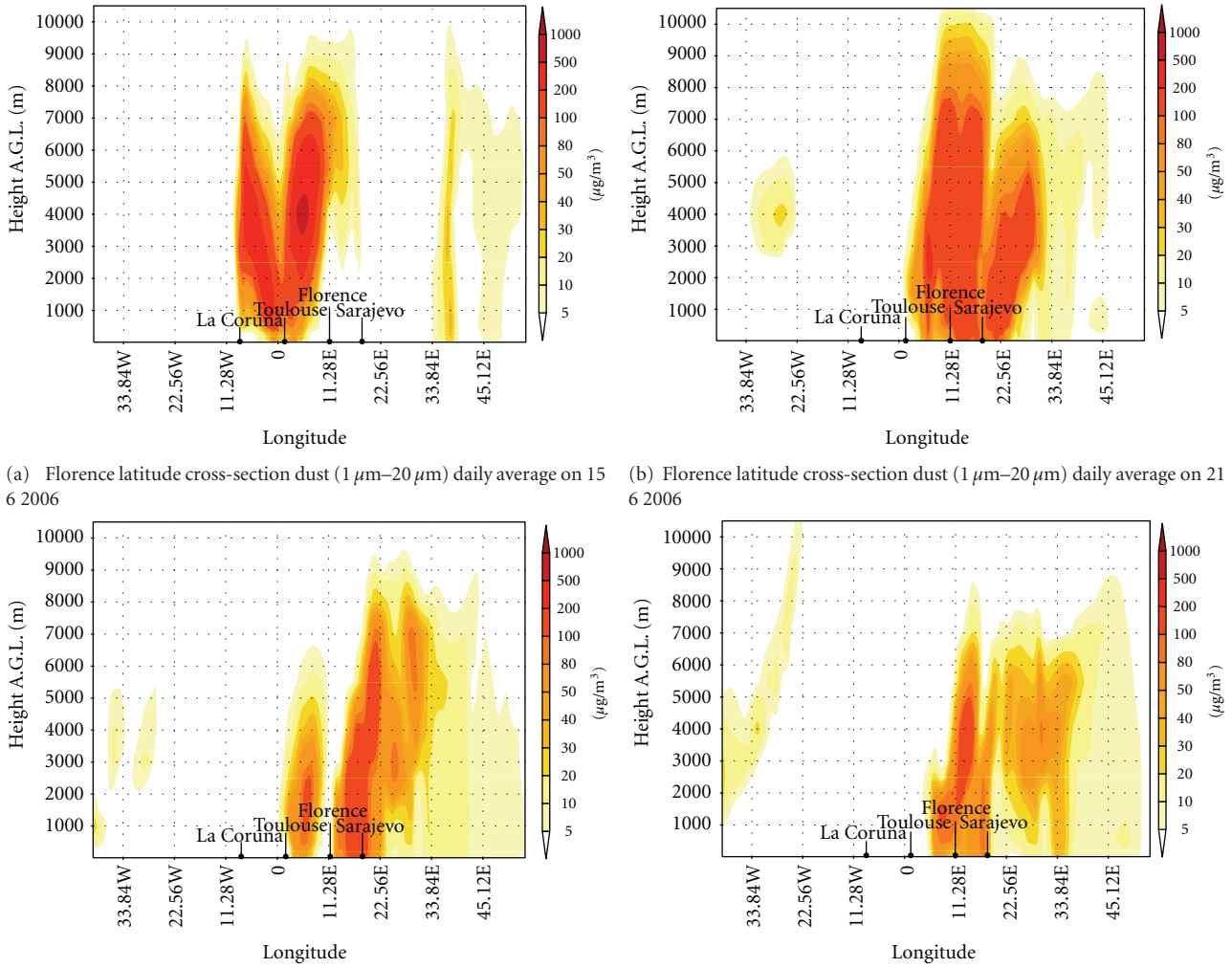

(a) Florence latitude cross-section dust (1 μm–20 μm) daily average on 15 6 2006

(b) Florence latitude cross-section dust (1 μm–20 μm) daily average on 21 6 2006

(c) Florence latitude cross-section dust (1 μm–20 μm) daily average on 24 6 2006

(d) Florence latitude cross-section dust (1 μm–20 μm) daily average on 26 6 2006

Figure 7: Latitude cross-section at 43.78°N of the daily average of dust concentration for 15th of June (a), 21st of June (b), 24th of June (c) and 26th of June 2006 (d).

concentration values are reported in Table 2. The Saharan dust contribution is quite high, with concentrations up to ~20 μg/m^3, and it can be considered the main cause of the PM_{10} 50 μg/m^3 limit value exceedances (values shown in bold in the table) occurring in this period.

3.4. Comparison between Model and Measurements. The comparison with in situ measurements plays a fundamental role for an evaluation of the model chain effectiveness in reproducing the deposition mechanism.

As explained in Section 3.3, the in situ measurements identify the dust outbreak from 18 June to 1 July, with a small residual contribution on 2 July. For the comparison, only three sites are used (Firenze, Capannori-Lucca, and Grosseto), as the relative sampling periods cover almost the entire extent of the episode.

In Figure 9, the time series of the daily simulated dust concentration at the ground level are compared with the Saharan dust contribution to the PM_{10} obtained by the measurements. Concerning the period extension, in the inland cities (Florence and Capannori-Lucca), the model simulation identifies the dust episode from 16 June to 2 July. The onset of the dust outbreak is thus anticipated in 2 days with respect to the measured data, while in the coastal city (Grosseto), the simulation and the measurements identify the same temporal range.

At all the sites, both the simulated and observed time series show a good agreement in the representation of the concentration decrease on 24-25 June and the following increasing phase up to the end of the episode.

Because the DUSTEM emission model provides particle sizes of 1–20 μm, the comparison with PM_{10} measurements is limited to a qualitative analysis and may lead to simulated concentration values that are higher than the soil dust concentrations obtained from the measurements. This behaviour may actually be observed in the inland cities. However, in the coastal cities, the simulation gives lower values than the measurements, which could be attributed to the model representation of the boundary layer's vertical extent, which could be underestimated near the coast,

Table 2: Saharan dust and PM_{10} concentrations, in $\mu g/m^3$, during the period of the Saharan intrusion of June 2006, for the six sampling sites ("—" indicates a contribution below the minimum detection limit).

	Firenze		Capannori		Grosseto	
	Saharan dust	PM_{10}	Saharan dust	PM_{10}	Saharan dust	PM_{10}
18/06/2006	2	22	2	24	—	18
19/06/2006	6	30	4	32	3	24
20/06/2006	14	42	9	38	5	27
21/06/2006	19	46	12	44	15	40
22/06/2006	**23**	**56**	14	48	**22**	**51**
23/06/2006	10	41	9	42	14	42
24/06/2006	8	42	6	45	3	31
25/06/2006	8	41	7	46	5	32
26/06/2006	12	44	8	40	9	37
27/06/2006	**13**	**50**	14	49	11	44
28/06/2006	**21**	**57**	**17**	**51**	**18**	**50**
	Arezzo		Prato		Livorno	
	Saharan dust	PM_{10}	Saharan dust	PM_{10}	Saharan dust	PM_{10}
30/06/2006	8	36	11	44	**19**	**50**
01/07/2006	4	15	2	25	6	40
02/07/2006	—	11	—	15	2	31

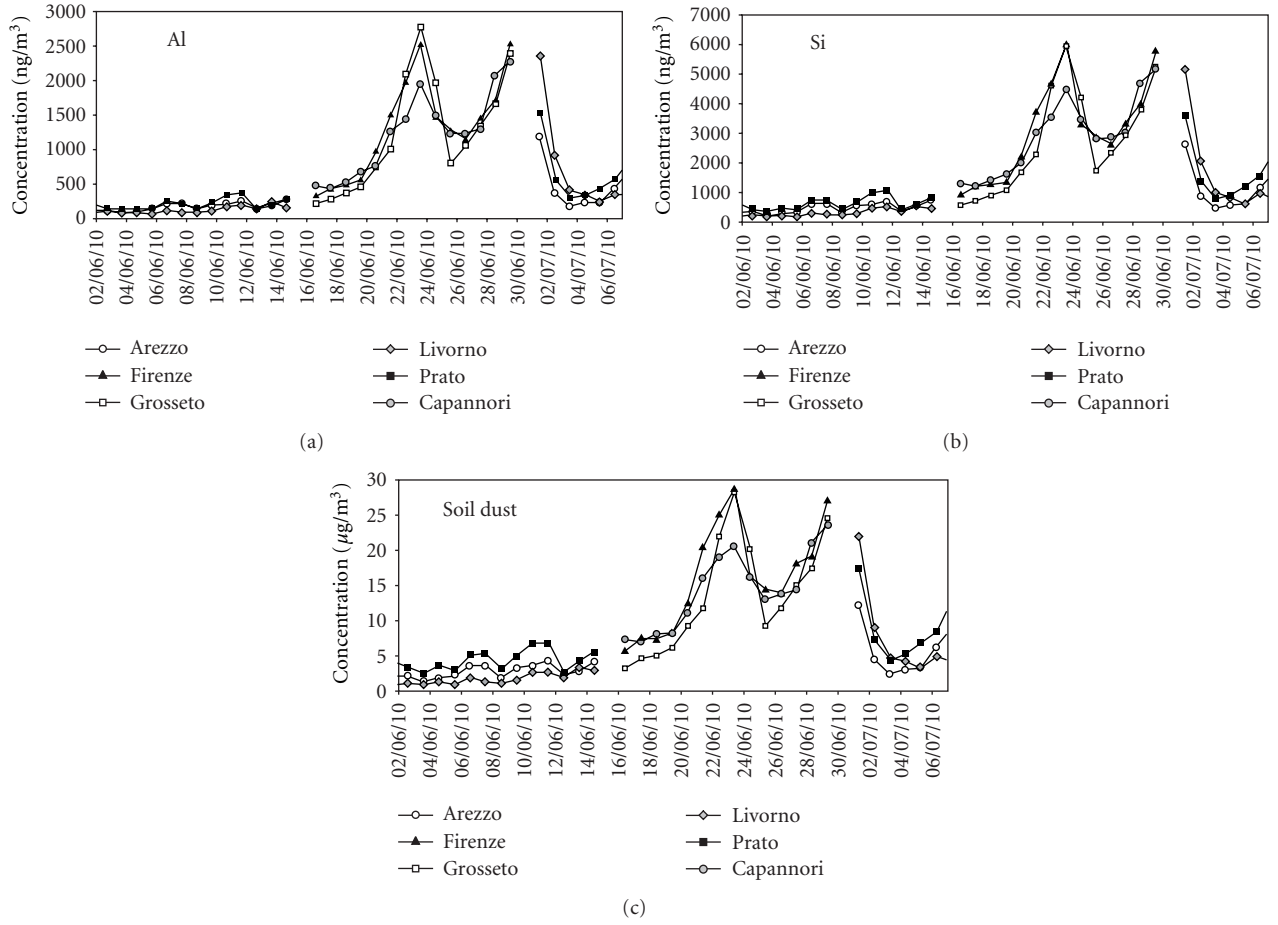

Figure 8: Daily concentrations of Al (ng/m^3), Si (ng/m^3), and soil dust ($\mu g/m^3$) in PM_{10} samples collected in June 2006 in six sampling sites in Tuscany (Italy).

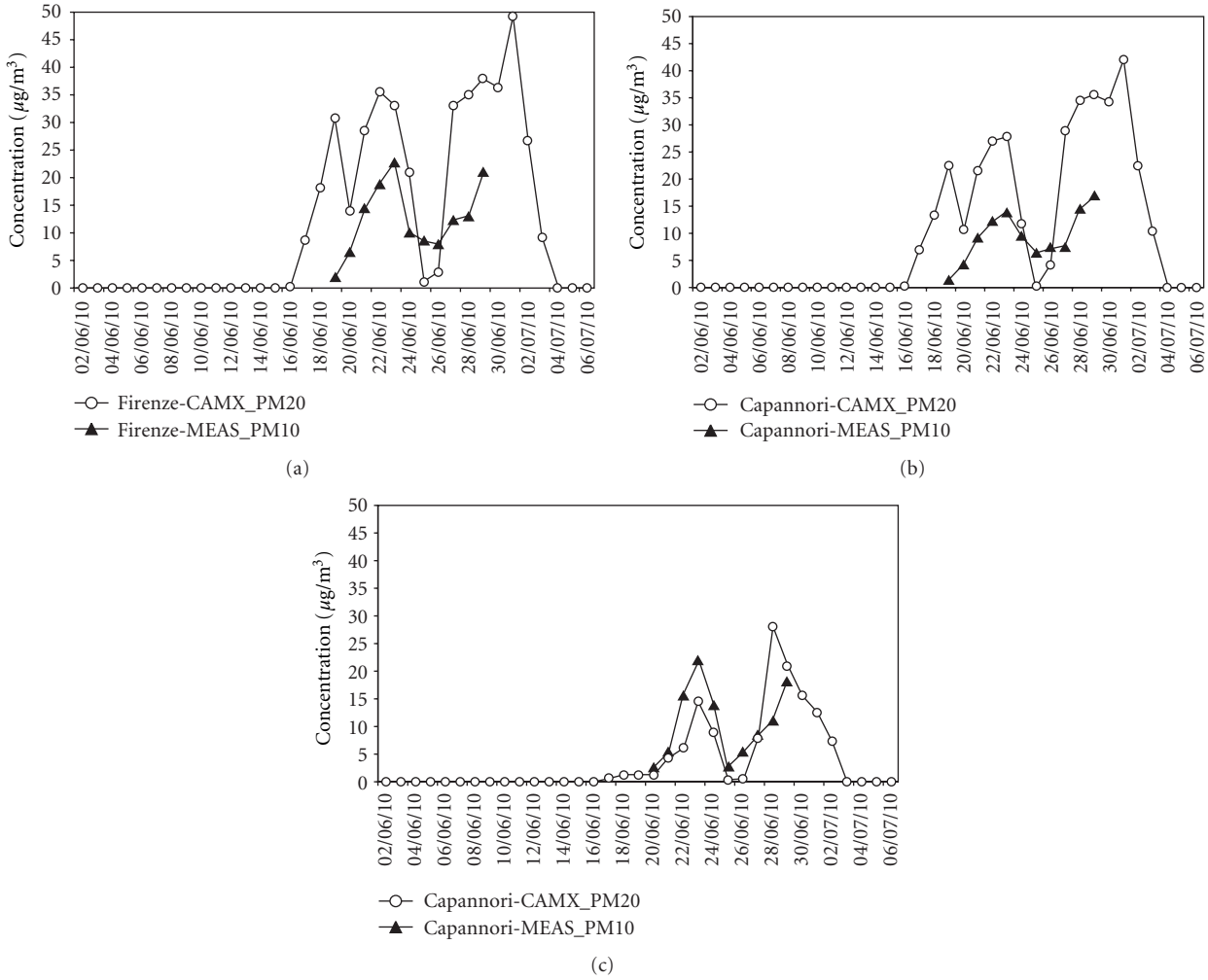

Figure 9: Comparison between mean daily modeled dust concentrations (CAMX_PM20) and Saharan dust contribution to PM_{10} obtained by ground measurements (MEAS_PM10), in Florence, Capannori-Lucca, and Grosseto (Tuscany, Italy).

obstructing the dust intrusions from higher to lower levels. The meteorological model RAMS has been configured with a horizontal and vertical resolution useful to reproduce the raising and transport phenomena, but it is not fine enough to describe the boundary layer near the coastline. Perhaps it will be necessary to introduce a finer nested grid into the meteorological model (and, consequently, the CAMx model) to describe the boundary layer with a better resolution over the target area.

4. Conclusions

Within the framework of the European Commission's guidelines to assess the natural contribution to PM_{10}, the aim of this work is to study the Saharan dust intrusions over the MB to quantify the dust impact at the ground level. The selected case study considers the large dust outbreak over the MB of June 2006. After a preliminary synoptic analysis, an ad hoc model chain is configured and physical-chemical analyses are conducted on PM_{10} samples collected in Central Italy. The model chain properly reproduces the dust emission and transport dynamics, as proved by comparison with available model maps. Furthermore, it describes the dust distribution on vertical profiles and the deposition at the ground level, adding detail to the satellite observations and optical thickness data analysis. Regarding ground-based measurements, the specific assessment of all the crustal elements by PIXE gives a more accurate quantitative estimate of the desert dust contribution than that obtained solely by PM_{10} mass concentration. The comparison between simulation results and specific insitu measurements shows a satisfying overall agreement, especially for the temporal evolution of the studied episode. Nevertheless, in the sampling site near the coast, the model simulation gives lower values than the measured ones. Near the coast, the model representation of the boundary layer's vertical extent could be underestimated, obstructing the dust intrusions to the ground level. To improve the performance of the model chain, it may be useful to introduce a nested grid in the meteorological model (and, consequently, in the CAMx model) with a higher resolution over the target area, where the measurement sites are located. However, the comparison

with PM_{10} measurements is limited to a qualitative analysis because the DUSTEM model provides emission rates for particle sizes of 1–20 μm. As a further development, the DUSTEM will be improved, taking into account a better soil type description to provide PM_{10} emission rates.

Acknowledgments

The authors would like to acknowledge the Tuscany Regional Government (Italy), which supported the PATOS project and provided the experimental data used here, and the support received within the CNR-Italy Short Term Mobility Program 2010. The authors would also like to acknowledge the NOAA Air Resources Laboratory for the provision of the HYSPLIT model results and NASA for the TOMS maps, satellite images, and the Giovanni online data system, developed and maintained by the NASA GES DISC for the dust maps used in this study.

References

[1] IPCC, "Changes in atmospheric constituents and in radiative forcing," in *Climate Change 2007: the Physical Basis*, P. Forster, V. Ramaswamy, P. Artaxo et al., Eds., pp. 129–234, Cambridge University Press, New York, NY, USA.

[2] J. Haywood and O. Boucher, "Estimates of the direct and indirect radiative forcing due to tropospheric aerosols: a review," *Reviews of Geophysics*, vol. 38, no. 4, pp. 513–543, 2000.

[3] J. E. Penner et al., "Aerosols, their direct and indirect effects," in *Climate Change 2001: the Scientific Basis*, J. T. Houghton, Y. Ding, D. J. Griggs et al., Eds., pp. 289–348, Cambridge University Press, Cambridge, UK, 2001.

[4] V. Ramaswamy et al., "Radiative forcing of climate change," in *Climate Change 2001: the Scientific Basis*, J. T. Houghton, Y. Ding, D. J. Griggs et al., Eds., pp. 349–416, Cambridge University Press, Cambridge, UK, 2001.

[5] U. Lohmann and J. Feichter, "Global indirect aerosol effects: a review," *Atmospheric Chemistry and Physics*, vol. 5, no. 3, pp. 715–737, 2005.

[6] IPCC, "Summary for policymakers," in *Climate Change 2007: the Physical Science Basis*, S. Solomon, D. Qin, M. Manning et al., Eds., Cambridge University Press, New York, NY, USA, 2007.

[7] N. M. Mahowald and L. M. Kiehl, "Mineral aerosol and cloud interactions," *Geophysical Research Letters*, vol. 30, no. 9, pp. 28–1, 2003.

[8] K. H. Rosenlof, S. J. Oltmans, D. Kley et al., "Stratospheric water vapor increases over the past half-century," *Geophysical Research Letters*, vol. 28, no. 7, pp. 1195–1198, 2001.

[9] T. D. Jickells, Z. S. An, K. K. Andersen et al., "Global iron connections between desert dust, ocean biogeochemistry, and climate," *Science*, vol. 308, no. 5718, pp. 67–71, 2005.

[10] G. S. Okin, N. Mahowald, O. A. Chadwick, and P. Artaxo, "Impact of desert dust on the biogeochemistry of phosphorus in terrestrial ecosystems," *Global Biogeochemical Cycles*, vol. 18, no. 2, Article ID GB2005, 9 pages, 2004.

[11] J. M. Prospero, P. Ginoux, O. Torres, S. E. Nicholson, and T. E. Gill, "Environmental characterization of global sources of atmospheric soil dust identified with the Nimbus 7 Total Ozone Mapping Spectrometer (TOMS) absorbing aerosol product," *Reviews of Geophysics*, vol. 40, no. 1, pp. 1–31, 2002.

[12] X. Tie, S. Madronich, S. Walters et al., "Assessment of the global impact of aerosols on tropospheric oxidants," *Journal of Geophysical Research D*, vol. 110, no. 3, pp. 1–32, 2005.

[13] J. M. Prospero, "Saharan dust transport over the North Atlantic Ocean and Mediterranean: an overview," in *The Impact of Desert Dust Across the Mediterranean*, S. Guerzoni and R. Chester, Eds., pp. 133–151, Kluwer Academic Publishers, 1996.

[14] U. Dayan, J. Heffter, J. Miller, and G. Gutman, "Dust intrusion events into the Mediterranean basin," *Journal of Applied Meteorology*, vol. 30, no. 8, pp. 1185–1199, 1991.

[15] X. Querol, J. Pey, M. Pandolfi et al., "African dust contributions to mean ambient PM10 mass-levels across the Mediterranean Basin," *Atmospheric Environment*, vol. 43, no. 28, pp. 4266–4277, 2009.

[16] S. Rodríguez, X. Querol, A. Alastuey, G. Kallos, and O. Kakaliagou, "Saharan dust contributions to PM10 and TSP levels in Southern and Eastern Spain," *Atmospheric Environment*, vol. 35, no. 14, pp. 2433–2447, 2001.

[17] M. Escudero, X. Querol, J. Pey et al., "A methodology for the quantification of the net African dust load in air quality monitoring networks," *Atmospheric Environment*, vol. 41, no. 26, pp. 5516–5524, 2007.

[18] B. Mason, *Principles of Geochemistry*, Wiley, New York, NY, USA, 1966.

[19] R. A. Pielke, W. R. Cotton, R. L. Walko et al., "A comprehensive meteorological modeling system-RAMS," *Meteorology and Atmospheric Physics*, vol. 49, no. 1-4, pp. 69–91, 1992.

[20] J. G. Acker and G. Leptoukh, "Online analysis enhances use of NASA Earth Science Data," *Eos*, vol. 88, no. 2, pp. 14–17, 2007.

[21] M. Chin, P. Ginoux, S. Kinne et al., "Tropospheric aerosol optical thickness from the GOCART model and comparisons with satellite and sun photometer measurements," *Journal of the Atmospheric Sciences*, vol. 59, no. 3, pp. 461–483, 2002.

[22] D. A. Gillette, "Major contributions of natural primary continental aerosols: source mechanisms," *Annals of the New York Academy of Sciences*, vol. 338, pp. 348–358, 1980.

[23] D. A. Gillette, "Production of dust that may be carried great distances," in *Desert Dust: Origin, Characteristics, and Effect on Man*, T. L. Pewe, Ed., vol. 186, pp. 11–26, Geological Society of America Special, 1981.

[24] B. Marticorena and G. Bergametti, "Modeling the atmospheric dust cycle: 1. Design of a soil-derived dust emission scheme," *Journal of Geophysical Research*, vol. 100, no. 8, pp. 16–430, 1995.

[25] F. Meneguzzo, M. Pasqui, G. Menduni et al., "Sensitivity of meteorological high-resolution numerical simulations of the biggest floods occurred over the Arno river basin, Italy, in the 20th century," *Journal of Hydrology*, vol. 288, no. 1-2, pp. 37–56, 2004.

[26] G. Messeri, A. Pellegrini, M. Pasqui et al., "Weather forecast using RAMS model. A case study," in *Proceedings of the Italian Physical Society Conference*, vol. 80, pp. 55–68, 2002.

[27] M. Pasqui, J. Lichtenegger, F. Meneguzzo, and G. Messeri, "Validation of Model rams with ERS-2 SAR observations in convectives storm events over the Mediterranean sea," in *Mediterranean Storms*, R. Deidda, A. Mugnai, and F. Siccardi, Eds., publicatioin no.2560, GNDCI, 2002.

[28] M. Pasqui, L. Bottai, C. Busillo et al., "Dust sandstorm dynamics analysis in northern China by means of atmospheric, emission, dispersion modeling," in *Proceeding of the 8th International Conference on Development of Drylands*, Beijing, China, 2006.

[29] M. Kanamitsu, W. Ebisuzaki, J. Woollen et al., "NCEP-DOE AMIP-II reanalysis (R-2)," *Bulletin of the American Meteorological Society*, vol. 83, no. 11, pp. 1631–1643, 2002.

[30] S. Nickovic, G. Kallos, A. Papadopoulos, and O. Kakaliagou, "A model for prediction of desert dust cycle in the atmosphere," *Journal of Geophysical Research D*, vol. 106, no. 16, pp. 18113–18129, 2001.

[31] I. Tegen and I. Fung, "Modeling of mineral dust in the atmosphere: sources, transport, and optical thickness," *Journal of Geophysical Research*, vol. 99, no. 11, pp. 22–914, 1994.

[32] E. Bartholomé and A. S. Belward, "GLC2000: a new approach to global land cover mapping from earth observation data," *International Journal of Remote Sensing*, vol. 26, no. 9, pp. 1959–1977, 2005.

[33] FAO, IIASA, ISRIC, ISSCAS, and JRC, "Harmonized world soil database," (version 1. 1), FAO, Rome, Italy and IIASA, Laxenburg, Austria, 2009.

[34] S. A. Slinn and W. G. N. Slinn, "Predictions for particle deposition on natural waters," *Atmospheric Environment. Part A*, vol. 14, no. 9, pp. 1013–1016, 1980.

[35] J. H. Seinfeld and S. N. Pandis, *Atmospheric Chemistry and Physics. from Air Pollution to Climate Change*, John Wiley and Sons, New York, NY, USA, 1998.

[36] P. Bonelli, G. M. Braga Marcazzan, and E. Cereda, "Elemental composition and air trajectories of African dust transported in Northern Italy," in *The Impact of Desert Dust Across the Mediterranean*, S. Guerzoni and R. Chester, Eds., pp. 275–283, Kluwer Academic Publishers, Dordrecht, The Netherlands, 1996.

[37] I. Borbely-Kiss, A. Z. Kiss, E. Koltay, G. Szabo, and L. Bozo, "Saharan dust episodes in Hungarian aerosol: elemental signatures and transport trajectories," *Journal of Aerosol Science*, vol. 35, no. 10, pp. 1205–1224, 2004.

[38] G. M. B. Marcazzan, P. Bonelli, E. Della Bella, A. Fumagalli, R. Ricci, and U. Pellegrini, "Study of regional and long-range transport in an Alpine station by PIXE analysis of aerosol particles," *Nuclear Inst. and Methods in Physics Research, B*, vol. 75, no. 1-4, pp. 312–316, 1993.

[39] M. Chiari, F. Lucarelli, F. Mazzei et al., "Characterization of airborne particulate matter in an industrial district near Florence by PIXE and PESA," *X-Ray Spectrometry*, vol. 34, no. 4, pp. 323–329, 2005.

[40] P. Formenti, M. O. Andreae, L. Lange et al., "Saharan dust in Brazil and Suriname during the Large-Scale Biosphere-Atmosphere Experiment in Amazonia (LBA)—cooperative LBA Regional Experiment (CLAIRE) in March 1998," *Journal of Geophysical Research D*, vol. 106, no. 14, pp. 14919–14934, 2001.

[41] G. Calzolai, M. Chiari, I. García Orellana et al., "The new external beam facility for environmental studies at the Tandetron accelerator of LABEC," *Nuclear Instruments and Methods in Physics Research, Section B*, vol. 249, no. 1-2, pp. 928–931, 2006.

[42] J. L. Campbell, N. I. Boyd, N. Grassi, P. Bonnick, and J. A. Maxwell, "The Guelph PIXE software package IV," *Nuclear Instruments and Methods in Physics Research, Section B*, vol. 268, no. 20, pp. 3356–3363, 2010.

[43] S. Becagli, C. Ghedini, S. Peeters et al., "MBAS (Methylene Blue Active Substances) and LAS (Linear Alkylbenzene Sulphonates) in Mediterranean coastal aerosols: sources and transport processes," *Atmospheric Environment*, vol. 45, no. 37, pp. 6788–6801, 2011.

[44] R. Washington, M. C. Todd, S. Engelstaedter, S. Mbainayel, and F. Mitchell, "Dust and the low-level circulation over the Bodélé Depression, Chad: observations from BoDEx 2005," *Journal of Geophysical Research D*, vol. 111, no. 3, Article ID D03201, 2006.

[45] C. Moulin, C. E. Lambert, F. Dulac, and U. Dayan, "Control of atmospheric export of dust from North Africa by the North Atlantic Oscillation," *Nature*, vol. 387, no. 6634, pp. 691–694, 1997.